

## Supplementary Information

### The landscape of human SVA retrotransposons

#### Authors

Chong Chu<sup>1</sup>, Eric W. Lin<sup>3,4</sup>, Antuan Tran<sup>1</sup>, Hu Jin<sup>1</sup>, Natalie I. Ho<sup>3,4</sup>, Alexander Veit<sup>1</sup>, Isidro Cortes-Ciriano<sup>2</sup>, David T. Ting<sup>3,4</sup>, Kathleen H. Burns<sup>5</sup>, Peter J. Park<sup>1\*</sup>

#### Affiliations

<sup>1</sup> Department of Biomedical Informatics, Harvard Medical School, Boston, MA, USA

<sup>2</sup> European Molecular Biology Laboratory, European Bioinformatics Institute, Hinxton, UK

<sup>3</sup> Massachusetts General Hospital Cancer Center, Harvard Medical School, Charlestown, MA 02129, USA

<sup>4</sup> Department of Medicine, Massachusetts General Hospital Harvard Medical School, Boston, MA 02114, USA

<sup>5</sup> Department of Pathology, Dana-Farber Cancer Institute, Harvard Medical School, Boston, MA 02215.

\* Correspondence should be addressed to P.J.P. ([peter\\_park@hms.harvard.edu](mailto:peter_park@hms.harvard.edu))

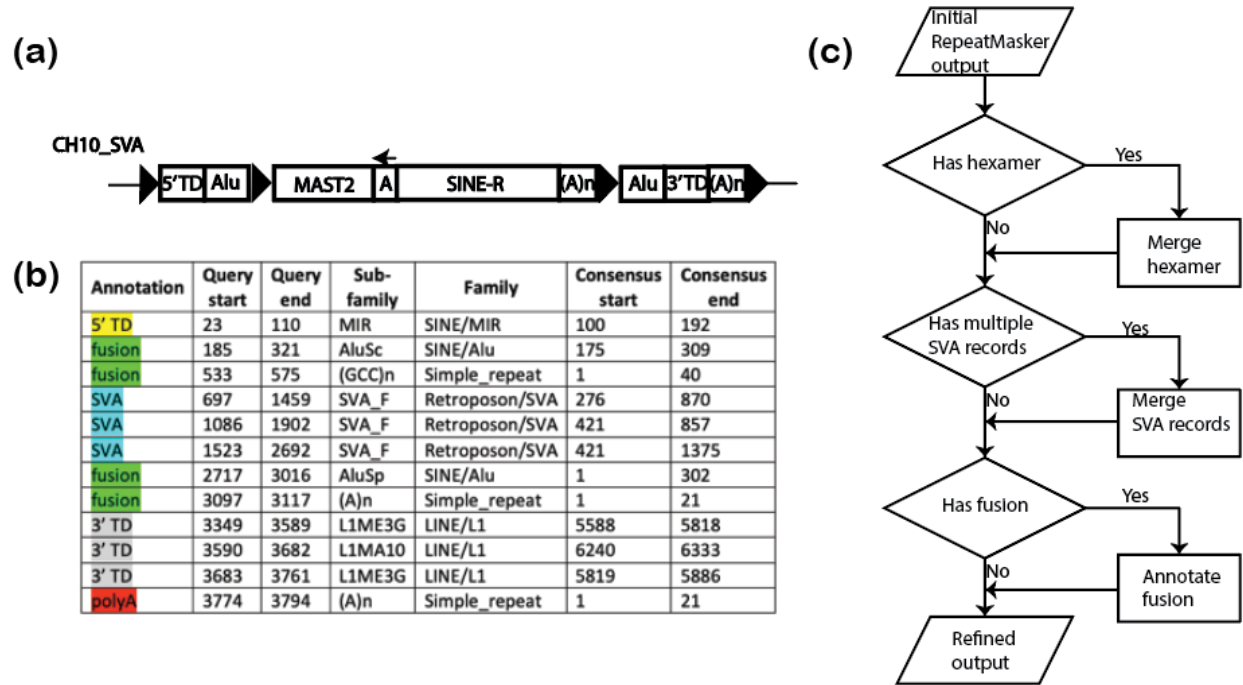


**Fig. S1: SVA retrotransposon annotation refinement.** a, The structure of the full length CH10\_SVA retrotransposon. Here, “TD” indicates transduction, and big triangles represent the “target-site-duplications”. b, RepeatMasker annotation of one CH10\_SVA copy. The whole copy is annotated to 12 records of several different types of subfamilies by RepeatMasker. c, the detailed procedure of the SVA annotation refinement module.

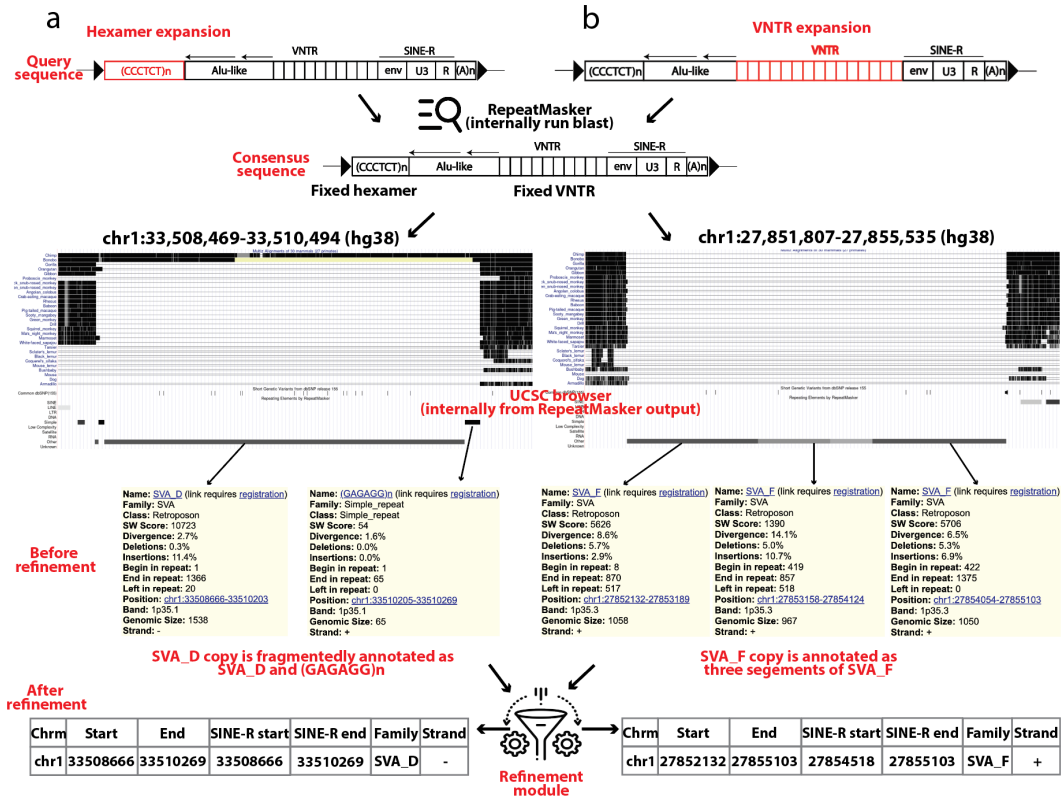


**Fig. S2: Example illustration of SVA annotation refinement.** a, RepeatMasker annotation of an SVA\_D retrotransposon breaks to two segments due to the hexamer expansion. With the refinement module the copy is annotated as an integrated copy. b, An SVA\_F copy is annotated to three segments by RepeatMasker because of the VNTR expansion. With the refinement module, the whole retrotransposon is annotated as an integrated copy.

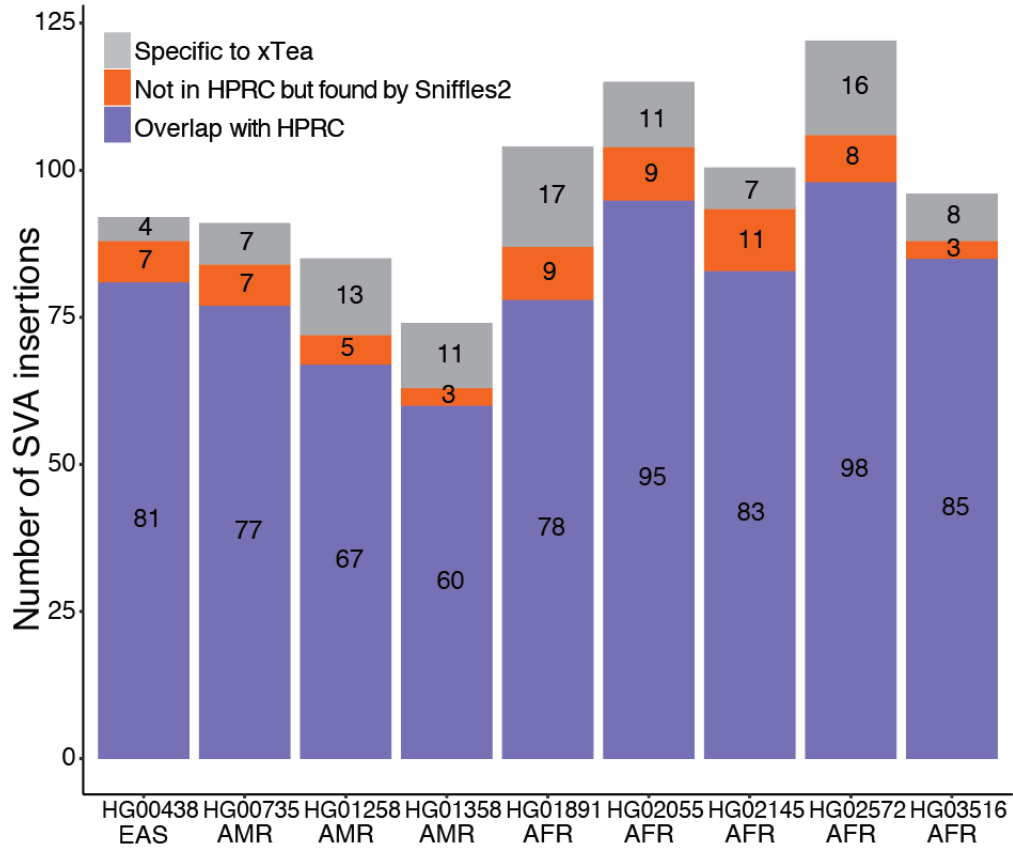
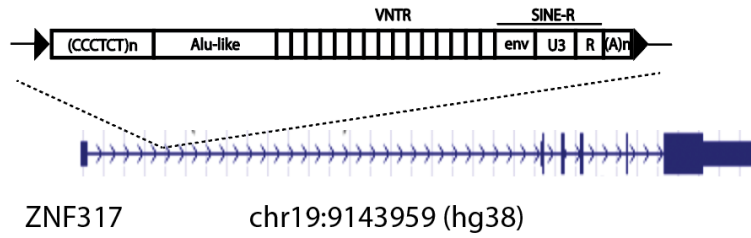


**Fig. S3: Number of benchmarked SVA insertions before filtering out low-mappability and segmental duplication region ones.** These are the same 9 samples on the same comparison as Fig. 2d, but here are the number of SVA insertions before filtering out those SVA insertions fallen into low-mappability and segmental duplication regions.



ZNF317 chr19:9143959 (hg38)  
 OCN\_AF: 0.1974,  
 and not detected in all other populations

**Fig. S4: An example of the population-specific SVA insertions.** This insertion is only reported in the Oceania population with a high population allele frequency of 0.1974. The insertion falls in an intronic region of gene *ZNF317*.

### SVA (polymorphic and reference) VS Gene Density

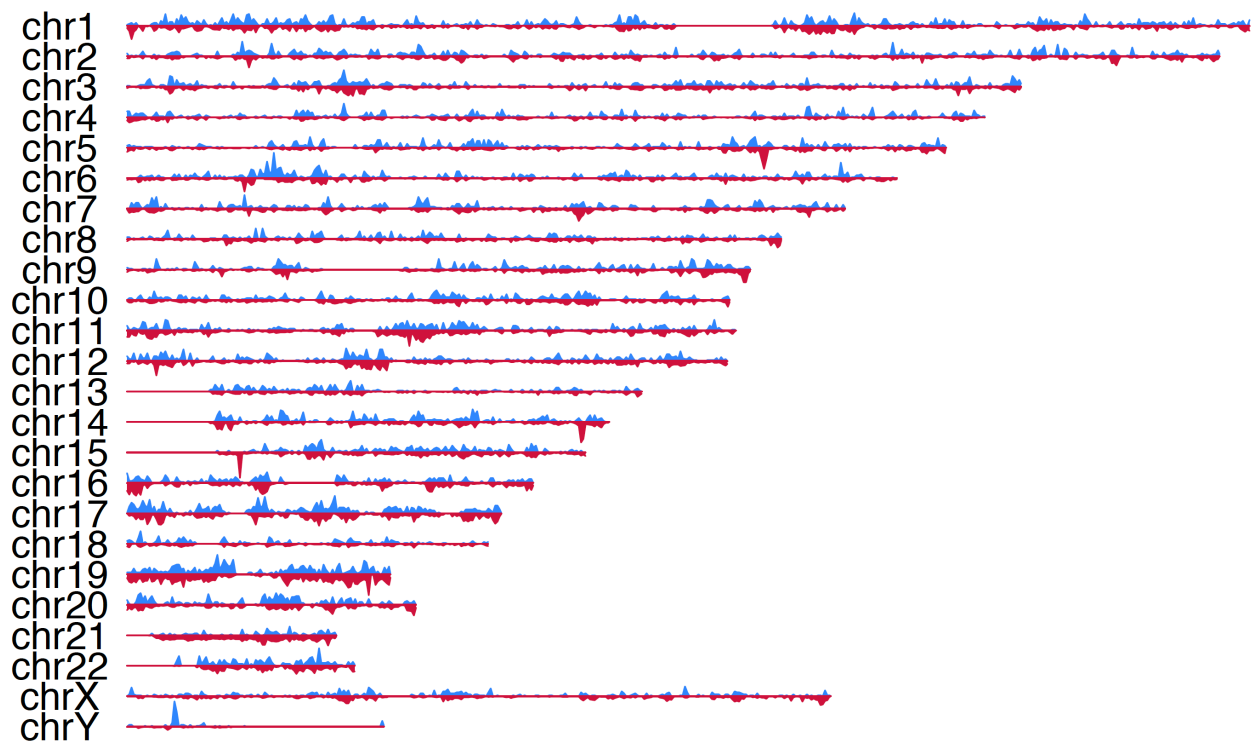


**Fig. S5: SVA and gene density distribution in the genome.** The top track (blue) shows the 5,107 reference and 8,505 polymorphic SVA copy distribution; the bottom track (dark red) shows the gene distribution (based on GENCODE Release 38).

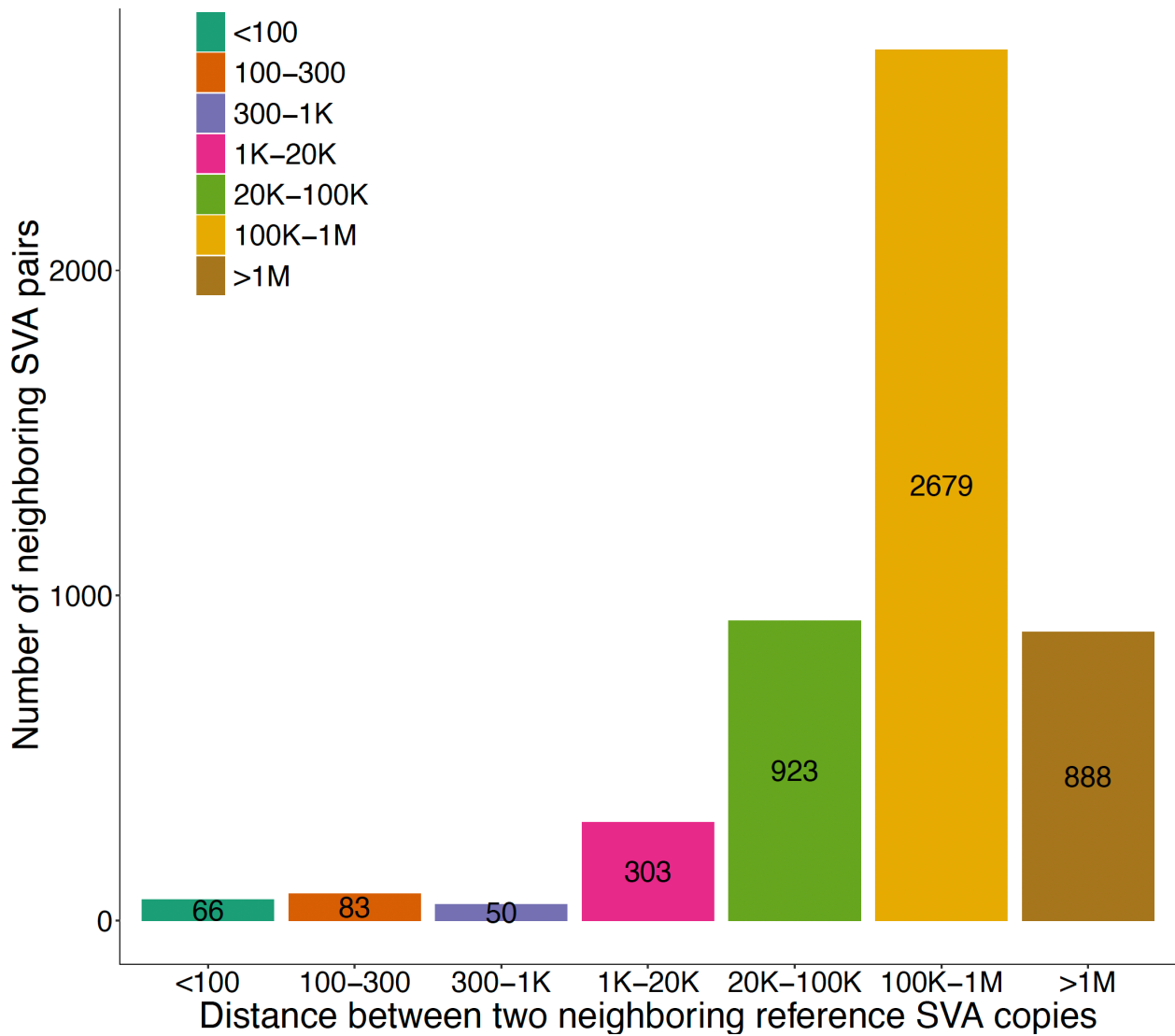


**Fig. S6: Distance distribution between each pair of neighboring reference SVA copies.** 199 (4.0%) are located within 1kb distance, 3,905 (78%) are situated within the range of 1 kilobase (kb) to 1 megabase (Mb), 888 (18%) extend beyond 1 Mb, while the remaining copies are found within 1 kb of each other.

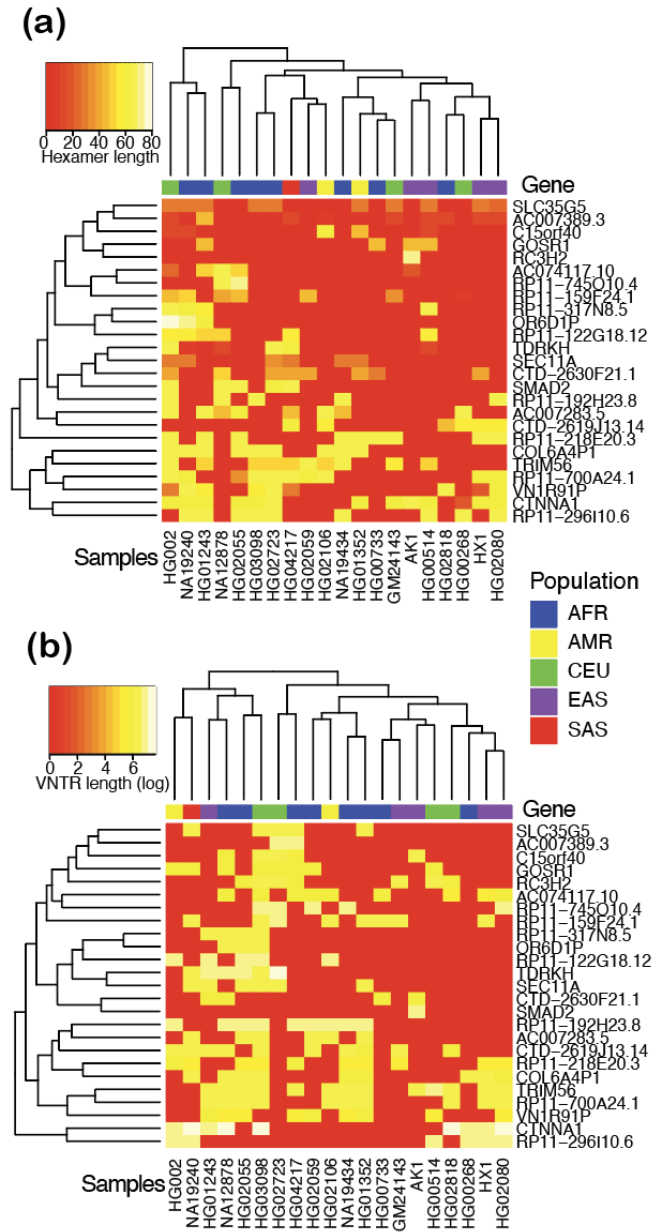


**Fig. S7: Hexamer and VNTR lengths at exonic regions.** The (a) hexamer and (b) VNTR lengths for the 25 reference SVA copies that fall in exonic regions are estimated for the 20 long-read samples. The variable expansion patterns suggest that both the hexamer and VNTR instances were expanded independently in the population.



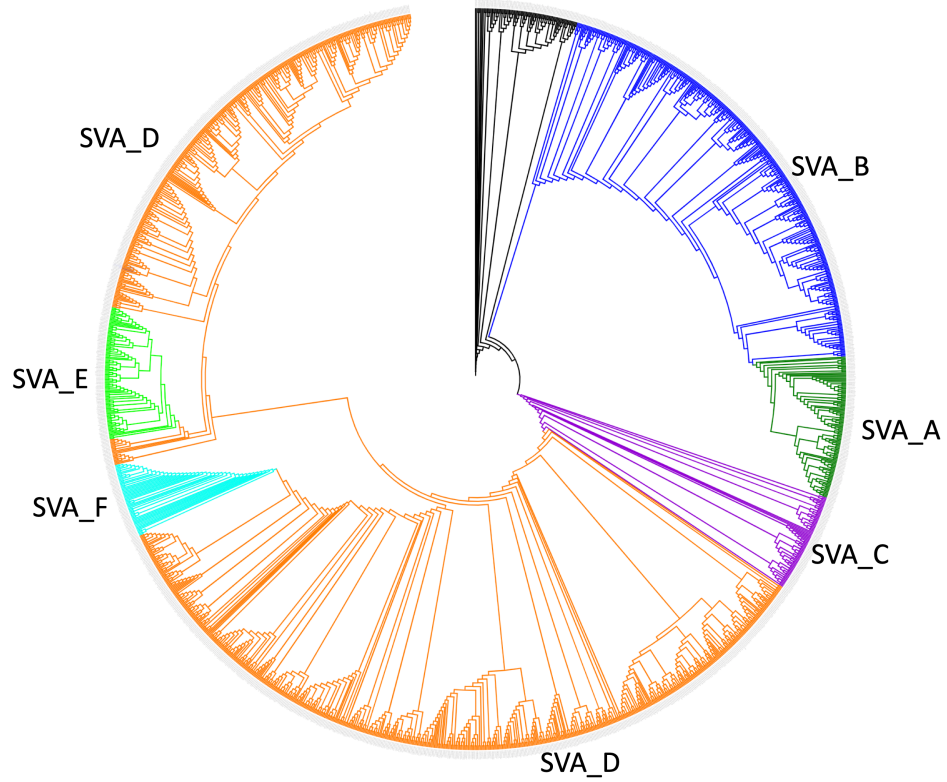


**Fig. S8: A phylogeny tree of 1,927 reference full-length SVA copies.** Subfamilies are annotated from the refinement module results. Different colors indicate different large branches. Copies annotated as the same subfamily are well-clustered. SVA\_E and SVA\_F appear to have evolved independently from different branches of the SVA\_D subfamily.

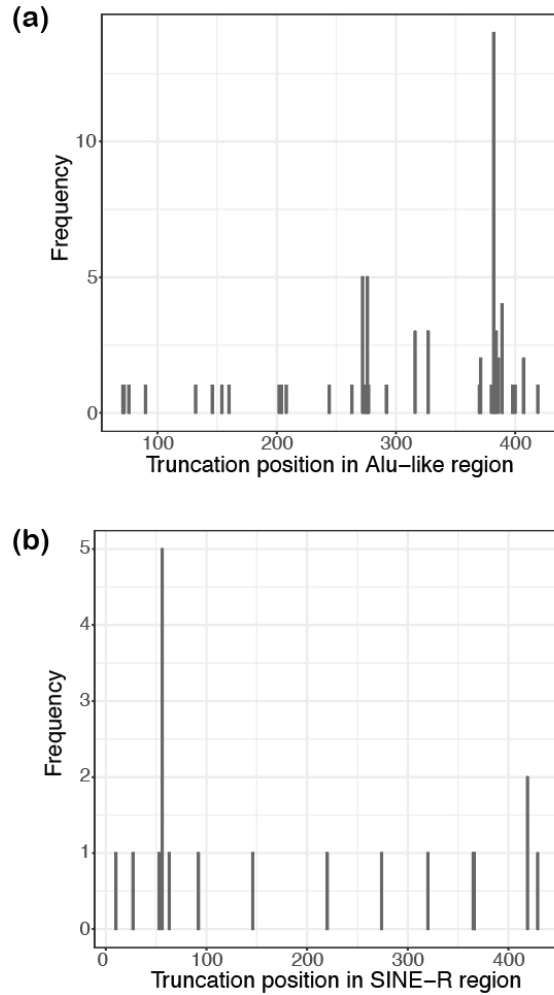


**Fig. S9: Number of truncated insertions by truncation position (Alu-like and SINE-R regions).** Truncated locations for all non-full-length SVA insertions identified from long read samples were checked, and the truncation position were counted for **(a)** Alu-like regions and **(b)** SINE-R regions.

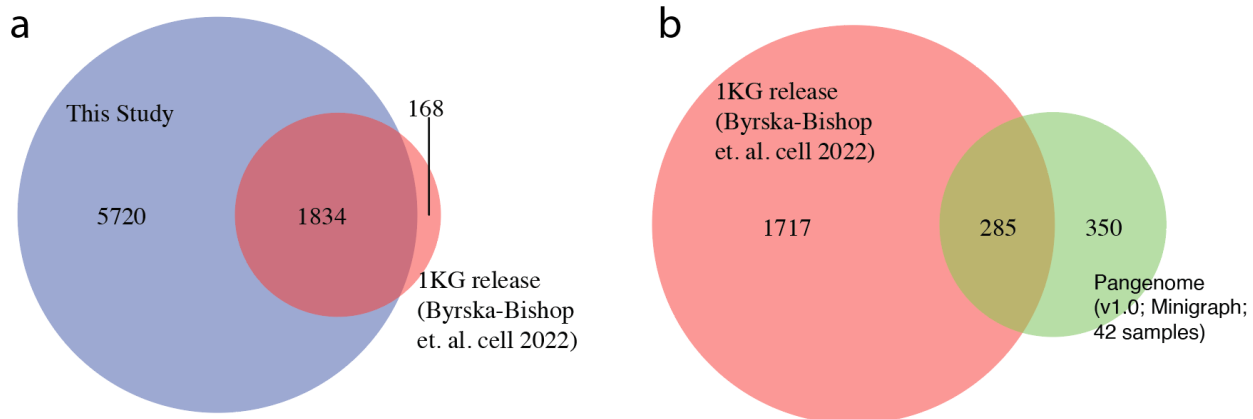


**Fig. S10: Comparison the Byrska-Bishop et. al. cell 2022 (1KG release) results with the results from this study and the results from pan-genome. a**, 1,834, 5,720, and 168 SVA insertions are overlapped, this study specific and 1KG release, respectively. **b**, 285, 1,717, 350 SVA insertions are shared, 1KG release specific and pan-genome specific, respectively.

Byrska-Bishop et. al. cell 2022  
on high-depth 1000 Genomes Project data  
(with GATK-SV)

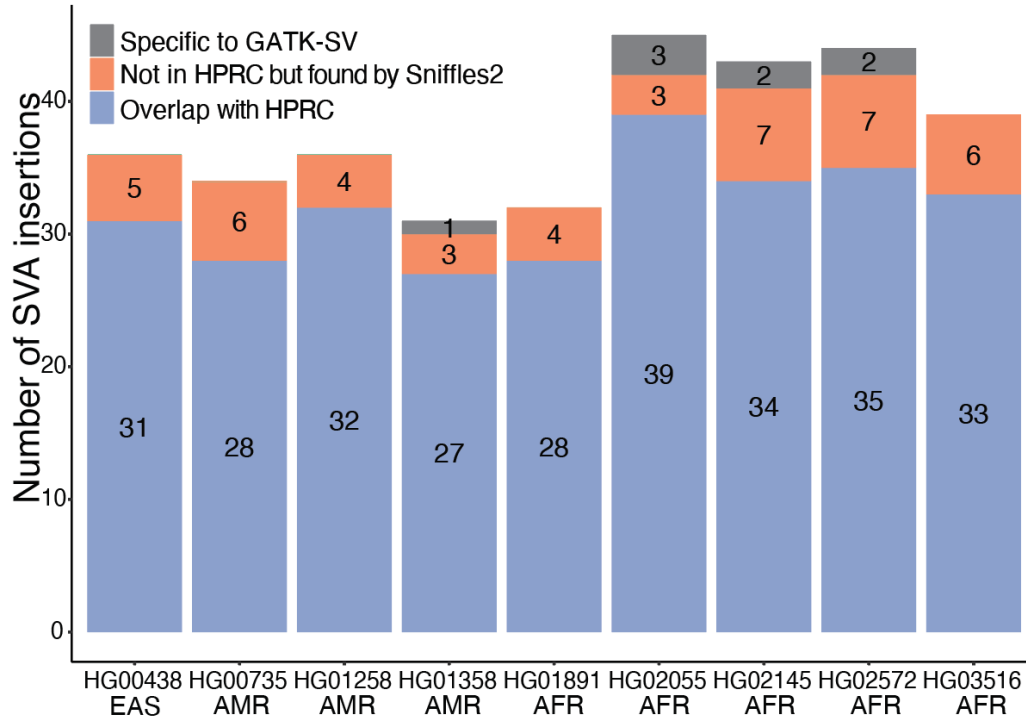


**Fig. S11: Benchmark GATK-SV pipeline in identifying SVA insertions with pan-genome and long-read caller Sniffles2.** We used the same 9 samples as used in Fig. 2d to evaluate the performance of GATK-SV. The number of overlapped SVA insertions with the pan-genome identified SVA insertions are shown in blue. For those not covered by the pan-genome results, we checked whether they are overlapped with the Sniffles2 results. The overlapped with Sniffles2 ones are shown in orange while the non-overlapped ones are shown in grey.

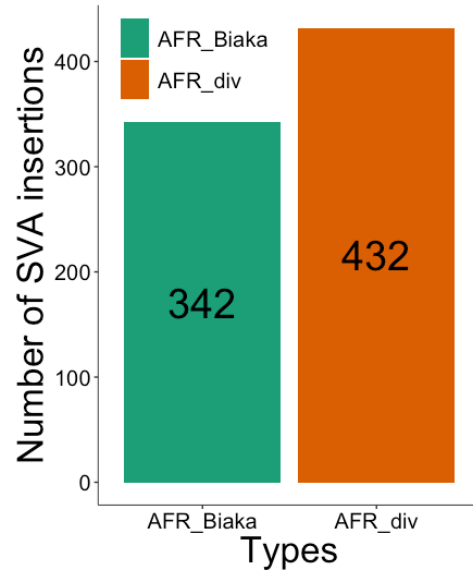


**Fig. S12: Comparison of the number of SVA insertions identified from two groups of samples of diverse and single population.** Each group is composed of 10 samples. All the samples of the first group (AFR\_Biaka) are from African Biaka population, while samples in the second group (AFR\_div) are from 10 different African populations. The number of identified SVA insertions are 342 and 432 for AFR\_Biaka and AFR\_div, respectively.

**Tab. S1 Primer pairs of each candidate SVA insertion of sample HG02145**

<b>HG02145 genomic region</b>	<b>Forward primer sequence (5'→3')</b>	<b>Reverse primer sequence (5'→3')</b>	<b>Expected size (bp)</b>
chr1:64384496	TTTCAGGGTAGGCAAAGCAGT	TCCCGGATGGCACGGC	844
chr3:147890048	TCCAGGCAATCTGGGTGGAT	CGAGGTTGGCCTGTTTCATTT	137
chr5:56152167	GCTTTTGTGCAAGCTACTGAACT	GCCTCCGCACAAACAAAAG	213
chr5:113114994	GATCACCAAGTACACAGGCACA	GGGTGGGCCCTCTGC	618
chr6:31329005	CTGCACTTGTACCCCTGAACT	CTGGGCTACAGAGTGAGACT	978
chr6:31329617	AGTCATCTGTCTGGTGGGTC	CAGTGGCCGGGTGGA	280
chr6:153108701	AATGGCAGAAATGGCACAGG	TTCTTTCGGAATGTAGGGGAAT	322
chr8:145028002	GTCTCTGAGTTCCCTCAGTTTT	AAATCAGATGGTTGCCGGGT	483
chr10:111843457	TGGCCTATCGCATTATCTTACAAA	TGCTGACCTTCCCTCCACTA	225
chr20:33285413	CCAAGTCTTGGAAGTTGCTA	ACCGTTTTAGCCGGGATG	262

**Tab. S2 Primer pairs of each candidate SVA insertion of sample HG02055**

<b>HG02055 genomic region</b>	<b>Forward primer sequence (5'→3')</b>	<b>Reverse primer sequence (5'→3')</b>	<b>Expected size (bp)</b>
chr4:56872286	CCTTCCACACCCAGCAATGT	TCCAGCTTTGGCTCGGCA	520
chr6:31329005	CTGCACTTGTACCCCTGAACT	CTGGGCTACAGAGTGAGACT	978
chr6:31329617	AGTCATCTGTCTGGTGGGTC	CAGTGGCCGGGTGGA	280
chr6:153108701	AAACACCAACAGGTGCATTAGC	TCTTTCGGAATGTAGGGGAATTTT	953
chr12:6139269	ACCCAAGGAAGTTGTTGCCT	CAGGATTCCAACCGCATTCA	374
chr15:65494012	CCAGCAGGGTAACCAAATACCT	TCATCACCATCCCTAATCTCAAGT	829
chr22:20648657	CACCAGAGACTCCCAACTGA	TTTCACCGTGTTAGCCAGGA	997

## References

1. Wang, T. et al. The Human Pangenome Project: a global resource to map genomic diversity. *Nature* 604, 437–446 (2022).
2. Li, H., Feng, X. & Chu, C. The design and construction of reference pangenome graphs with minigraph. *Genome Biol.* 21, 265 (2020).
3. Smit, A. F. A., Hubley, R. & Green, P. RepeatMasker Open-4.0. 2013--2015. Preprint at (2015).
4. Smolka, M. et al. Comprehensive Structural Variant Detection: From Mosaic to Population-Level. *bioRxiv* 2022.04.04.487055 (2022) doi:10.1101/2022.04.04.487055.